

Unravelling the Origins of Ice Nucleation on Organic Crystals

Gabriele C. Sosso,¹ Thomas F. Whale,² Mark A. Holden,³ Philipp Pedevilla,⁴ Benjamin J. Murray,² and Angelos Michaelides⁴

¹*Department of Chemistry and Centre for Scientific Computing, University of Warwick, Gibbet Hill Road, Coventry CV4 7AL, United Kingdom^a*

²*Institute for Climate and Atmospheric Science, School of Earth and Environment, University of Leeds, Leeds LS2 9JT, United Kingdom*

³*School of Earth and Environment and School of Chemistry, University of Leeds, Leeds LS2 9JT, United Kingdom*

⁴*Thomas Young Centre, London Centre for Nanotechnology and Department of Physics and Astronomy, University College London, Gower Street London, London, WC1E 6BT, UK*

Organic molecules such as steroids or amino acids form crystals that can facilitate the formation of ice – arguably the most important phase transition on earth. However, the origin of the ice nucleating ability of organic crystals is still largely unknown. Here, we combine experiments and simulations to unravel the microscopic details of ice formation on cholesterol, a prototypical organic crystal widely used in cryopreservation. We find that cholesterol – which is also a substantial component of cell membranes – is an ice nucleating agent more potent than many inorganic substrates, including the mineral feldspar (one of the most active ice nucleating material in the atmosphere). Scanning electron microscopy measurements reveal a variety of morphological features on the surfaces of cholesterol crystals: this suggests that the topography of the surface is key to the broad range of ice nucleating activity observed (from -4 to -20 C°). In addition, we show via molecular simulations that cholesterol crystals aid the formation of ice nuclei in a unconventional fashion. Rather than providing a template for a flat ice-like contact layer (as found in the case of many inorganic substrates), the flexibility of the cholesterol surface and its low density of hydrophilic functional groups leads to the formation of molecular cages involving both water molecules and terminal hydroxyl groups of the cholesterol surface. These cages are made of 6- and, surprisingly, 5-membered hydrogen bonded rings of water and hydroxyl groups that favour the nucleation of hexagonal as well as cubic ice (a rare occurrence). We argue that the phenomenal ice nucleating activity of steroids such as cholesterol (and potentially of many other organic crystals) is due to (i) the ability of flexible hydrophilic surfaces to form unconventional ice-templating structures and (ii) the different nucleation sites offered by the diverse topography of the crystalline surfaces. These findings clarify how exactly organic crystals promote the formation of ice, thus paving the way toward the understanding of ice formation in soft and biological matter - with obvious reverberations on atmospheric science and cryobiology.

I. INTRODUCTION

The freezing of liquid water into crystalline ice is a ubiquitous phenomenon which is part of our everyday experience¹ and has countless reverberations in fields as diverse as cryobiology^{2–4} and atmospheric science^{5,6}. Strikingly, the overwhelming majority of ice on earth forms heterogeneously, i.e. thanks to the presence of substances, other than water itself, which facilitate the ice nucleation process^{5,7}. Much of what is known about heterogeneous ice nucleation has come from the study of atmospherically relevant ice nucleating agents⁵: in fact, heterogeneous ice nucleation from supercooled water plays a critical role in the glaciation of mixed phase clouds, which in turn influences the climate^{8,9}. A variety of substances are known to nucleate ice efficiently in the atmosphere, including inorganic species such as silver iodide¹⁰, feldspar^{11–13} as well as biological entities such as the bacterium *pseudomonas syringae*^{14–16} or birch pollen¹⁷.

Biological ice nucleating agents also play a key role

in the ever-growing field of cryobiology: in fact, the formation of ice in biological matter is the cornerstone of cryotherapy and cryopreservation^{4,18}, i.e. the long-term storage of frozen biological material which is essential to enable cutting-edge technologies such as regenerative medicine^{19,20}. A number of organic crystals have been known to facilitate ice nucleation^{21,22}, and molecular crystals of steroids such as cholesterol (CHL)²³ are used to boost the formation of ice when cryopreserving biological material^{2,24}. Importantly, CHL molecules also represent a major component (up to 40%) of animal cell membranes²⁵, thus prompting the question of whether this steroid can play a role as ice nucleator in the context of ice formation in biological matter.

However, the microscopic details of heterogeneous ice nucleation on CHL – and indeed on the vast majority of organic and inorganic compounds alike – remain remarkably poorly understood⁷, although a substantial body of experimental work has been devoted to assess the ice nucleation ability of biological matter^{22,26–32}. In fact, the reason why many biological ice nucleating agents display a far stronger ice nucleating activity than most inorganic materials^{5,7} is still largely unknown. Partly this is because obtaining molecular-level insight into the nucleation process is still a formidable challenge for ex-

^a) Electronic mail: G.Sosso@warwick.ac.uk

periments, and only very recently simulations of heterogeneous ice nucleation have become feasible^{7,13,33–40}, largely thanks to the capabilities of the coarse grained mW water model⁴¹. Indeed mW has played a pivotal role in enabling systematic investigations of ice nucleation on e.g. carbonaceous⁴² or hydroxylated organic surfaces⁴³. However, fully atomistic water models and enhanced sampling methods are often required to take into account the subtleties of the hydrogen bond network between water and complex impurities^{44,45}.

In this work, we bring together experiments and simulations to take an ambitious step forward in furthering our understanding of ice formation on organic crystals. We focus on CHL, due to its relevance in cryopreservation and its role within cellular membrane, unravelling microscopic motivations for heterogeneous ice nucleation likely to be shared by many other organic crystals. We find via micro-litre droplet nucleation measurements (μ -NIPI) that CHL crystals display an outstanding ice nucleation ability (stronger than most inorganic ice nucleating agents), with freezing events initiating at very mild supercooling $\Delta T_S = T_{\text{Melt}} - T = 4$ K down to $\Delta T_S = 20$ K. Scanning electron microscopy suggests that the activity of these crystals as ice nucleating agents across such a wide temperature range could be due to the diverse topography of the surface of the cholesterol crystals, which are likely to offer a variety of different nucleation sites. In order to get a molecular-level insight into the mechanism of ice formation on CHL crystals, we harness enhanced sampling simulations, focusing on the hydroxylated (001) face of cholesterol monohydrate (CHLM) – the most relevant surface (and polymorph, as discussed below) in biological scenarios. We find that CHL crystals facilitate the formation of ice in a non-conventional fashion: in contrast to what has been observed in the case of inorganic substrates such as e.g. carbonaceous particles⁴² or clay minerals⁴⁵, the flexibility of the CHLM surface and the large spacing of its hydroxyl groups prevent the formation of a flat, ice-like layer of water molecules at the water-crystal interface. Instead, the hydroxyl groups participate in the formation of 5- and 6-membered hydrogen bonded rings of water molecules forming peculiar molecular “cages” that provide an effective template for the nucleation of *both* cubic and hexagonal ice (a rare occurrence).

As a whole, our findings suggest that the formation of ice on CHL crystals originates from the ability of their flexible hydrophilic surfaces to trigger the formation of unconventional ice-templating molecular features. In addition, different nucleation sites potentially offered by the diverse topography of the crystal can further enhance the intrinsic ice nucleation potential of CHL surfaces. This insight could help to understand ice formation on a number of other organic compounds, from amino acid crystals^{46,47} to bacterial fragments^{48,49} – as they are all characterised by the presence of flexible hydrophilic surfaces displaying diverse topological features. In addition, organic crystals such as cholesterol are positioned “in between” inorganic and biological ice nucleating agents: they possess the order and the crystalline surfaces of the former, and the complexity and flexibility of the latter. This work thus paves the way to a molecular-level under-

standing of ice formation in biological matter, tackling a substrate (CHL crystals) that embeds unique features of very different classes of materials.

II. METHODS

μ L-NIPI experiments and scanning electron microscopy measurements

The ice nucleation efficiency of CHLM was evaluated using an adapted version of the μ L Nucleation by Immersed Particles Instrument (μ L-NIPI) described in detail in Ref.⁵⁰. To make the flat plates we dissolved 2g of pure CHL (Sigma Aldrich) in approximately 30 ml of hot (~ 343 K) 95% ethanol (Sigma-Aldrich). The CHL solution was then allowed to cool slowly, causing crystallisation of large (up to approx. 1 cm across) flat plates of CHLM. Individual plates of CHLM of around 2mm diameter were then recovered by vacuum filtration on a filter membrane and placed onto a thin (~ 0.1 mm) glass plate. The glass plate was then placed onto an EF600 Stirling cryocooler. A Picus Biohit electronic pipette was then used to deposit 1 μ l droplets of MilliQ water onto the separated CHLM plates. The EF600 cryocooler was then used to reduce the temperature of the droplets at a rate of 1 K/min. freezing was monitored using a camera. In this way the droplet fraction frozen curve presented in Fig. 1a was built up. The data is the result of several cooling runs as only about 10 droplets could be frozen per experiment. It was important that plates were not in contact as ice clearly propagated across the CHL surface, triggering neighbouring droplets after an initial freezing events, when multiple droplets were placed on a single plate.

In order to calculate the (surface) density of the active ice nucleation sites (n_s , commonly used to compare the ice nucleating efficiency of different substances⁵) on the CHLM surface (reported in Fig. 1) we have used the following expression:

$$\frac{n(T)}{N} = 1 - \exp[-n_s(T) A], \quad (1)$$

where $n(T)$ is the number of droplets frozen at temperature T , N is the total number of droplets in the experiment and A is the surface area of nucleating agent per droplet. The value of A for each droplet was measured using the image analysis software imageJ, customarily used to quantify particles size in biosciences⁵¹. The resulting estimate of the mean value of A is 1.82 ± 0.46 mm².

The uncertainties associated with the values of n_s have been calculated using Monte-Carlo simulations of possible active ice nucleation sites distributions, propagated with the uncertainty associated with A – as described in Harrison et al.¹². These simulations generate a list of possible values for the number of active sites per droplet for a given experiment, given the observed freezing data. By repeating this process a great many times, a distribution of the possible active site distributions that can

account for the freezing of each droplet is obtained. The error bars for the CHLM n_s data reported in Fig. 1 are generated by propagating this distribution with the uncertainty in surface area of cholesterol per droplet and taking the 95% confidence interval of the resulting distribution. At high and low temperature ends of the reported data, where the Poisson uncertainty (i.e. the error originating from the Monte-Carlo simulations) is largest, the contribution of the uncertainty in surface area amounts to approximately 25% of total uncertainty in $n_s(T)$, with the Poisson uncertainty in the active site distribution accounting for the remainder of the error bars.

Scanning electron microscopy (SEM) was performed on CHLM plates. These were mounted on copper tape, then coated with 2 nm of iridium. SEM was performed with an FEI Nova NanoSEM 450 in high vacuum mode, using an Everhart-Thornley Detector (ETD).

Molecular dynamics simulations

The computational setup we have used is depicted in Fig. 3a. A single layer of CHL molecules, cleaved along the (001) plane (perpendicular to the normal to the slab) was prepared by starting from the experimental cell parameters and lattice positions⁵². Specifically, a CHLM crystal system made of two mirroring slabs (intercalated by water molecules, in a ratio of 1:1) was cleaved along the (001) plane. The triclinic symmetry of the system (space group $C1$) was preserved, and we have constructed a 3 by 3 supercell with in-plane dimensions of 37.17 and 36.57 Å. We positioned 1923 water molecules randomly atop this CHLM slab at the density of the TIP4P/Ice model⁵³ at 300 K, and expanded the dimension of the simulation cell along the normal to the slab to 100 Å. This setup allows for a physically meaningful equilibration of the water at the density of interest at a given temperature, but suffers from two distinct drawbacks: i) the CHLM slab possesses a net dipole moment which is not compensated throughout the simulation cell and ii) the presence of the water-vacuum interface can alter the structure and the dynamics of the liquid film. However, we have previously addressed these issues in previous work dealing with the hydroxylated (001) polar surface of the clay mineral kaolinite^{44,45}, concluding that such details do not affect the mechanism nor the kinetics of ice formation. In addition, the water film is thick enough to allow a bulk-like region to exist in terms of both structure and dynamics. The effect of the water-vacuum interface is therefore negligible. The slab considered in this work presents the hydrophilic, -OH terminated heads of the CHL molecules to the water, in agreement with experimental insight⁵⁴. As we discuss in the main text, the interaction between the hydroxyl groups (which display amphoteric characteristics in terms of the hydrogen bond network) of CHL molecules and water is responsible for the templating effect of CHLM crystals which serves to promote ice nucleation.

The CHARMM36⁵⁵ force field was used to model the CHL crystals, taking advantage of a recent update of this force field parameters explicitly with respect to CHL⁵⁶.

In order to mimic the experimental conditions, we have constrained the system at the experimental lateral dimensions (detailed together with the computational geometry in the SI), and we have also restrained the positions of the hydrophobic tail of each CHL molecule (specifically, the carbon atoms C25, C26 and C27, see the inset of Fig. S1 in the SI) by means of an harmonic potential characterised by a spring constant of 10000 kJ/mol. All the other atoms within the CHLM slab are unconstrained. We have verified that the thermal expansion of the crystal at 230 K ($\sim 0.1\%$ with respect to each lateral dimension) does not alter the structure nor the dynamics of the water-kaolinite interface. This setup is thus as close as we can get to the realistic (001) hydrophilic surface of CHLM within the CHARMM36 model. Implications of the flexibility of the CHLM slab are discussed in the SI. The interaction between the water molecules have been modelled using the TIP4P/Ice model⁵³, so that our results are consistent with the homogeneous simulations of Ref. 57. The interaction parameters between the clay and the water were obtained using the standard Lorentz-Berthelot mixing rules⁵⁸.

Extreme care must be taken in order to correctly reproduce the structure and the dynamics of the water-CHLM interface. The Forward Flux Sampling (FFS) simulations reported in this work rely on a massive collection of unbiased Molecular Dynamics (MD) runs, all of which have been performed using the GROMACS package, version 4.6.7. The code was compiled in single-precision, in order to alleviate the huge computational workload needed to converge the FFS algorithm and because we have taken advantage of GPU acceleration, which is not available in the double-precision version. The equations of motions were integrated using a leap-frog integrator with a time step of 2 fs. The van der Waals (non bonded) interactions were considered up to 10 Å, where a switching function was used to bring them to zero at 12 Å. Electrostatic interactions have been dealt with by means of an Ewald summation up to 12 Å. The NVT ensemble was sampled at 230 K using a stochastic velocity rescaling thermostat⁵⁹ with a very weak coupling constant of 4 ps in order to avoid temperature gradients throughout the system. The geometry of the water molecules (TIP4P/Ice being a rigid model) was constrained using the SETTLE algorithm⁶⁰ while the P-LINCS algorithm⁶¹ was used to constrain the O-H bonds within the clay. We have verified that these settings reproduce the dynamical properties of water reported in Ref.⁵⁷. The system was equilibrated at 300 K for 10 ns, before being quenched to 230 K over 50 ns. This is the starting point for the calculation of the initial flux rate for the FFS algorithm, which lasted about 1.5 μ s and thus allowed us to investigate the water-CHLM interface as well (see e.g. Fig. 3).

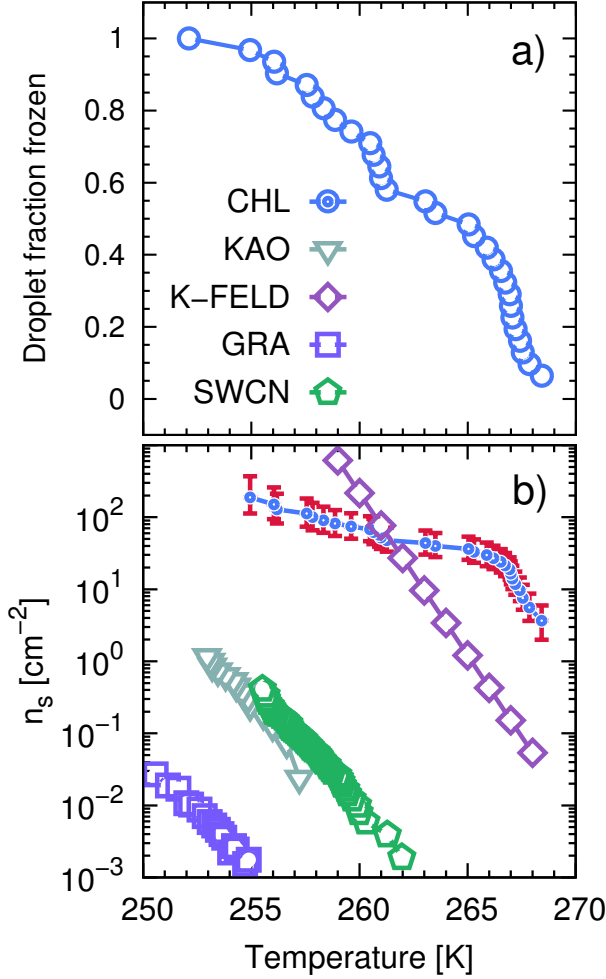


FIG. 1. *CHLM crystals promote the formation of ice across a wide range of temperatures.* (a) Droplet fraction frozen as a function of temperature for 1 μ l water droplets placed onto a CHLM substrate. (b) Ice-active surface site density n_s (see text and Methods section) values for the same data reported for CHLM (CHL) in panel (a), together with n_s values for kaolinite (KAO) from Herbert *et al.*⁶², BCS376 feldspar (K-FELD) from Atkinson *et al.*¹¹, graphene oxide (GRA) from Whale *et al.*⁶³ and single-walled carbon nanotubes (SWCN) also from Ref. 63. The uncertainty in terms of temperature associated with the CHLM data is ± 0.4 K.

III. RESULTS

A. Cholesterol promotes the formation of ice across a wide range of temperatures

We start by experimentally investigating the ice nucleating ability of cholesterol crystals - as a function of supercooling. CHL can crystallise into two different polymorphs, namely anhydrous⁶⁴ (CHLA) and CHLM⁵². The latter is the most relevant to ice formation, as it spontaneously forms in aqueous environments^{52,54,65–68}. Conveniently, CHLM crystallises from a mixture of 95% ethanol and 5% water as plates with the (001) surface forming the flat surface of the plates⁶⁶. The platy crystal habit of CHLM is characteristic of CHLM as opposed to CHLA, which tends to crystallise as needles.

CHLM crystals display a layered structure: bilayers of CHL molecules are stacked along the [001] direction, and facile cleavage along the (001) planes leads to surfaces exposing either a $-\text{CH}_3$ terminated, hydrophobic surface or a $-\text{OH}$ terminated, hydrophilic surface. Atomic and chemical force microscopy measurements indicate that in aqueous and organic solution conditions, the hydrophilic (001) surface is most abundantly found, in the form of largely homogeneous crystalline faces⁵⁴. Early experimental evidence suggested substantial ice nucleation activity of CHLM at very mild supercooling ($\Delta T_S = 5$ K)^{21,23,69}. The ice nucleation efficiency of CHLM was evaluated using an adapted version of the μ l-Nucleation by Immersed Particles Instrument (μ l-NIPI) experiments μ l-NIPI described in detail in Ref. 50. Experiments were performed by placing droplets directly onto a surface of crystalline CHLM. We used an electronic pipette to place 1 μ l droplets of water onto the (001) plane of plates of CHLM. The water droplets were then cooled down at a rate of 1 K/min and freezing monitored using a camera. In this way the fraction of frozen droplets can be determined as a function of temperature. Note that as the crystalline surface is submerged in liquid water these experiments are conducted at 100% relative humidity - i.e. in "immersion mode"⁷⁰.

In Fig. 1a we report the fraction of frozen droplets as a function of temperature for CHLM. It can be seen that CHLM can induce ice nucleation at temperatures as warm as 269 K. This agrees with previous studies which have reported high nucleation temperatures for CHL in the immersion mode^{2,24}. In here, we investigate the ice nucleating ability of CHLM as a function of supercooling. As shown in Fig. 1a, the spread of nucleation temperatures for the CHLM sheets is very broad, with some of them freezing at temperatures as low as 252 K. To allow for a comparison of the efficiency of ice nucleation by CHLM with other known nucleating species we have calculated the ice-active surface site density (n_s) for CHLM on the basis of the size of the contact patch of the water droplets with the CHL plates. As explained in greater detail in the Methods section, n_s is a site specific measure of ice nucleation efficiency which does not take into account the time dependence of ice nucleation, on the basis that the impact of time dependence on heterogeneous ice nucleation is generally minimal^{62,70,71}. We have compared the ice nucleating efficiency of CHLM with that of e.g. kaolinite powder⁶², which has commonly been regarded as an efficient ice nucleating agent in the past⁷² and of BCS 376 feldspar powder, which is known to nucleate ice highly efficiently¹¹ and was likely responsible for earlier observations of efficient ice nucleation in kaolinite samples. It can be seen that CHLM nucleates ice far more efficiently than kaolinite and more efficiently even than the feldspar at warm temperatures. Thus, CHLM has the potential to be a highly efficient ice nucleating agent in immersion mode across a wide range of temperatures - which is the scenario typically encountered when dealing with cryobiological applications.

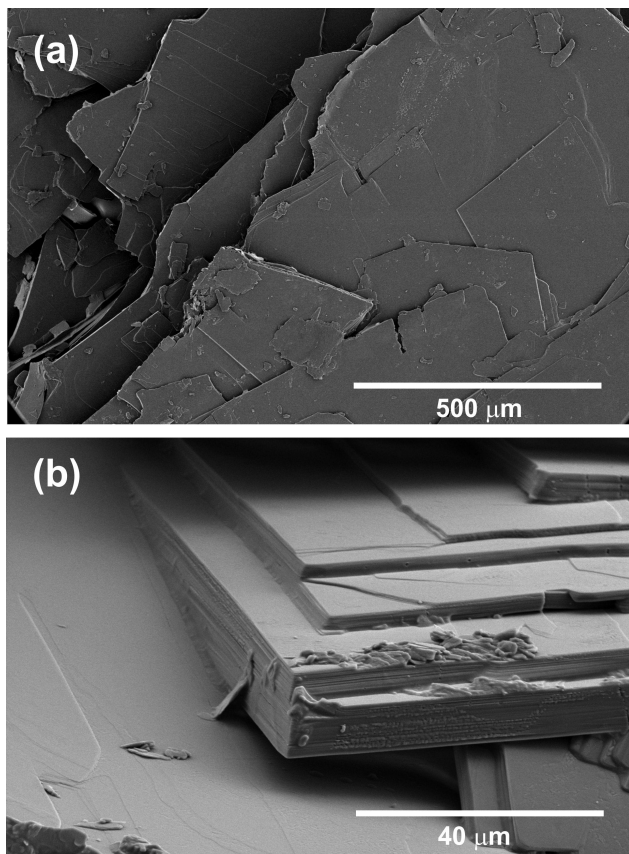


FIG. 2. *CHLM crystals display a diverse surface topography.* SEM images of CHLM crystals, which predominantly expose {001} surfaces – consistent with what has been reported in Ref. 54. It is quite clear that these plates possess numerous topographical features, particularly steps and terraces.

B. The role of surface topography

As noted above the spread of freezing temperatures we report for CHLM is very broad. This behaviour suggests that the nucleation behaviour of CHLM is spatially heterogeneous, i.e. different parts of the surface nucleate ice with differing efficiency. This is commonly known as site specific nucleation behaviour^{62,70,71,73}, and it can be appreciated to a lesser extent for the other ice nucleating agents considered in Fig. 1b. However, it is interesting to note that CHLM crystals seem to lead to two different ice nucleation regimes, as can be inferred from Fig. 1b (note the two different slopes characterising n_s as a function of temperature). As it is becoming increasingly clear that the topography of the ice nucleating agents must play an important role in the heterogeneous nucleation of ice from liquid water^{40,74,75}, we suspect that structural differences between the crystalline areas covered by the water droplets are responsible for the wide spread in nucleation temperatures observed. This hypothesis is supported by the scanning electron microscope (SEM) images of the (001) face of CHLM reported in Fig. 2. While the crystalline plates appear as mostly flat and smooth within the resolution of $\sim 100 \mu\text{m}$, it is clear that there exist numerous defects, particularly steps and terraces, which can potentially present opportunities for

complicated surface geometries to occur. How exactly the nanometric structure of crystalline ice nucleating agents affects the kinetics of ice formation is still an open question (see e.g. Refs. 32,40). In fact, it would be expected that an atomically smooth and homogeneous CHL surface would nucleate ice with a single nucleation rate and hence within a far narrower range of temperatures than that reported in Fig. 1. The role of specific defects and broadly speaking of the surface morphology to ice formation on CHL – and the vast majority of biological nucleating agents, it thus remains yet to be fully understood. For instance, it is not immediately clear why CHLM crystals are much more effective than feldspar in promoting the formation of ice. In the next section, we will address this issue by showing that in addition to the topography of the surface, the formation of a peculiar hydrogen bond network at the water-CHLM interface is key in determining the ice nucleating ability of this compound.

C. The cholesterol-water interface

In order to investigate the molecular-level details of the CHLM-water interface, we have performed unbiased molecular dynamics simulations at strong supercooling ($\Delta T_S = 42 \text{ K}$) employing the CHARMM36^{55,56} and the TIP4P/Ice⁵³ force fields for CHL and water molecules respectively. Computational details and results concerning the validation of our computational setup are reported in the Methods section and in the Supplementary Information (SI) respectively, while the computational geometry is depicted in Fig. 3a.

A water slab ($\sim 40 \text{ \AA}$ thick) is in contact with the hydroxylated (001) surface of CHLM ($\text{CHLM}_{001}^{-\text{OH}}$), modelled as a single layer of CHL molecules. This surface is hydrophilic, due to the presence of amphoteric hydroxyl groups. As CHL molecules are relatively bulky and the crystal is held together by weak electrostatic interactions only, the arrangement of these -OH groups on the CHLM surface is characterised by a broad distribution of large OH-OH distances, ranging from 5.1 to 7.1 \AA – as illustrated in Fig. 3a. Such a pattern of hydroxyl groups does not straightforwardly match any particular low-index Miller surface of either hexagonal or cubic ice. This is relevant, as a good structural match between a substrate and ice³⁸ has traditionally been considered as a “requirement” of an effective ice nucleating agent⁷⁶.

Interestingly, despite the presence of the hydroxyl groups, the density profile of the oxygen atoms of the water molecules on CHLM reported in Fig. 3b resembles that for water at hydrophobic walls⁷⁷. The enhancement ($\sim 30\%$ in Fig. 3b) of the density, within the first peak of the profile, compared to its value in the bulk of the water slab, is much smaller than that (typically a factor four or six) observed for e.g. water in contact with hydrophilic walls – or indeed water on kaolinite. This is because, the outer layer of the CHLM crystals is much more mobile/flexible than that of kaolinite: this is not surprising, as we are comparing a molecular organic crystal (held together by van der Waals interactions) with a (covalently bonded) clay mineral. Importantly, it is rea-

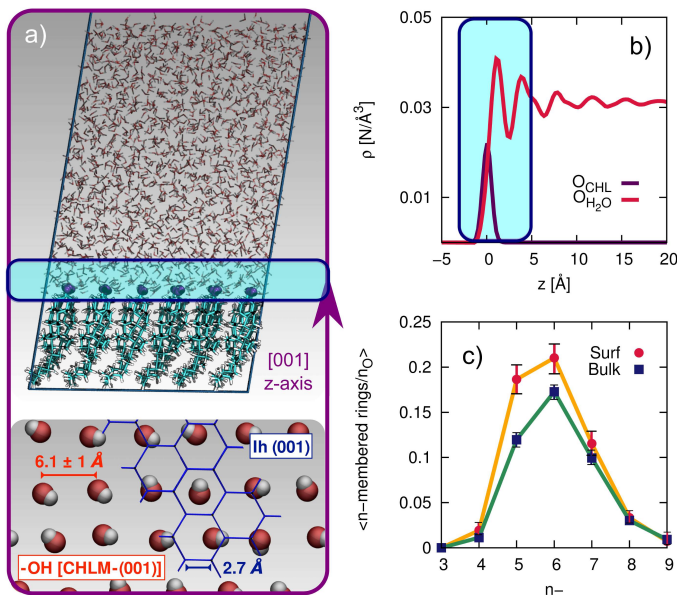


FIG. 3. *Structuring of water on the (001) hydroxylated face of CHLM.* a) Representative snapshot of a molecular dynamics simulation of a water slab in contact with the (001) hydroxylated face of CHLM. The inset at the bottom illustrates the arrangement of the hydroxyl group on the CHLM surface; an hypothetical ice I_h (001) plane (blue) is superimposed on part of the image to highlight the absence of a structural match between -OH groups and ice. b) Density profile of oxygen atoms belonging to either the -OH hydroxyl groups of CHLM molecules (O_{CHL}) or water molecules (O_{H_2O}) along the z -axis parallel to [001] direction, thus normal to the water-CHLM interface. The zero of the x -axis corresponds to the average position of the O_{CHL} atoms, while the shaded area in green identifies the water-CHLM interface. Statistics have been accumulated over a 1.5 μ s long simulation at 230 K. c) Number of n -membered rings of hydrogen bonded water molecules at the water-CHLM interface (Surf) or within the bulk of the water slab (Bulk), normalised by the number of oxygen atoms in each region. Note that at the water-CHLM interface oxygen atoms belonging to the CHLM -OH hydroxyl groups have also been considered when computing the rings statistics.

sonable to assume that a similar degree of flexibility characterises the majority of organic crystals containing long molecules such as steroids. This is relevant to ice formation because, as discussed in e.g. Ref. 43, the structural fluctuations of organic/biological ice nucleating particles can strongly affect the kinetics of ice nucleation. In fact, we have shown in Ref. 45 that the same argument holds in the case of kaolinite as well: for instance, a “frozen” kaolinite surface (atoms are kept fixed during MD simulations) leads to nonphysically fast ice nucleation rates.

Because of this flexibility of the CHL molecules and the low-density of hydroxyl groups at the water-CHLM interface, we did not observe (within a 200 ns time scale) the formation of an ordered, ice-like over-layer of water molecules, in contrast with what is generally found in the case of idealised crystalline surfaces⁷⁸, carbonaceous particles⁴² or kaolinite crystals^{44,45}. In fact, most inorganic substrates are characterised by surfaces where atomic/molecular species are tightly packed, and can thus potentially provide a high density of functional

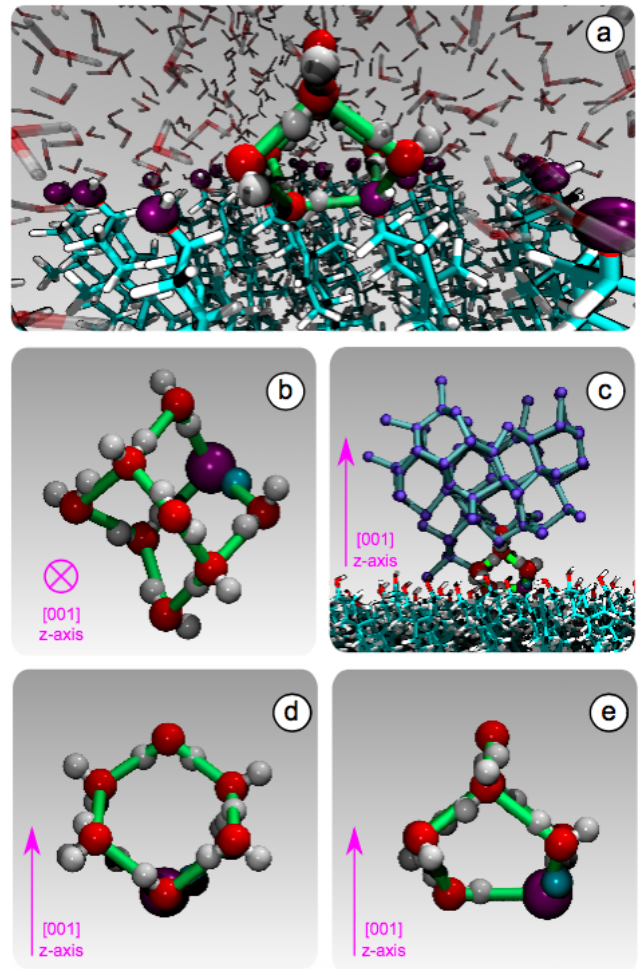


FIG. 4. *The formation of unconventional ice-templating molecular structures: hydrogen bonded cages.* a) A hydroxyl group (purple) of CHLM participates into a hydrogen bonded cage of water molecules. b) A single hydrogen bonded cage (top view), which constitutes the building block of cubic ice (panel c, side view). Note that these cages are made of both 6-membered (panel d, side view) and 5-membered (panel e, side view) hydrogen bonded rings, involving water molecules as well as a hydroxyl group provided by the CHLM surface.

groups for supercooled water to interact with, typically by forming a more or less ordered overlayer sitting on top of the crystalline surface. In the case of the water-CHLM interface, however, water molecules can partially infiltrate the outer layer of the CHLM surface (see Fig. 3a and Fig. 3b) due to the relatively large spacing between the CHL molecules and the flexibility of the surface itself. As a net result, despite the absence of a flat overlayer of ice-like water molecules, the amphoteric character of the hydroxyl groups does facilitate the formation of a network of hydrogen bonded rings of water molecules as well as hydroxyl groups, as illustrated in Fig. 3c. In particular, we observe the emergence of 6-membered rings of hydrogen bonded water molecules and hydroxyl groups. These rings are the building blocks of both hexagonal (ice I_h) and cubic (ice I_c) ice, and are the most abundant species in bulk water. Note that the occurrence of these rings is actually even more pronounced in the proximity of the CHLM-water interface (red/orange points/curve

in Fig. 3c). Surprisingly, there is also an increase in the number of 5-membered water/hydroxyl rings at the crystal-liquid interface. Pentagonal rings are thought to frustrate the homogeneous formation of ice⁷⁹; however, in this case both 6- and 5-membered rings alike contribute to the formation of ice-like fluctuations such as the "cage" shown in Fig. 4a. These cages are indeed the building blocks of ice I_c (see Fig. 4b and Fig. 4c), and involve hydrogen bonds between water molecules and hydroxyl groups, as depicted in Fig. 4d and Fig. 4e. Thus, in this heterogeneous nucleation scenario, the presence of 5-membered rings is not detrimental; on the contrary, they lead to the formation of ice-like fluctuations of the water network at the water-CHLM₀₀₁^{OH} interface.

We note that the emergence of these cages is the reason why we have chosen to consider as the "interfacial layer" those water molecules within 5.0 Å from the average position of the oxygens of the CHL hydroxyl groups - as illustrated by the shaded region in Fig. 3b. As shown in e.g. Ref. 80, the definition of this water layer can have an impact on the analysis of the structure of - in this case - the water-CHLM interface. While the interfacial layer can be chosen on the basis on indicators such as the first or second minimum of the density profile (see Fig. 3b), we have found that the rather generous cutoff of 5.0 Å is sufficient to accommodate the substantial extent of the hydrogen bonded cages depicted in Fig. 4d and Fig. 3e. We have also verified that by choosing the second minimum of the density profile ($\sim 7\text{\AA}$) our results, including the trends within the rings statistics reported in Fig. 3c, are basically unchanged.

Our findings thus contribute the growing body of evidence^{40,43,78} that the structural mismatch argument alone cannot be deemed as neither a sufficient nor a necessary criteria to assess, let alone to predict, the ice nucleating ability of a given substrate³⁸. This is bound to be especially true in the case of biological ice nucleating agents such as macromolecules¹⁷, where the notion itself of a lattice mismatch is ill defined. In fact, we argue that organic crystals such as cholesterol lie halfway in between inorganic (e.g. mineral crystals) and biological (e.g. bacterial fragments) ice nucleating agents, as they are characterised by the relatively flat and (in this case) -OH regularly patterned surfaces of the former while showing the flexibility of the latter. This is particularly relevant for CHL, which is a substantial component of animal cellular membranes²⁵ and could thus contribute to promote the heterogeneous formation of ice in biological matter - a possibility we will investigate in future work. In this respect, it is interesting to note that very recent simulations⁸¹ suggest that ice can bind to antifreeze proteins via "anchored clathrate" motifs not dissimilar to the molecular cages discussed above.

D. Ice nucleation mechanism and kinetics

In order to characterise the mechanism as well as the kinetics of ice nucleation on CHLM₀₀₁^{OH} we have performed forward flux sampling (FFS) simulations⁸²⁻⁸⁹. While other enhanced sampling techniques are in prin-

ciple available, such as metadynamics⁹⁰, transition path sampling⁹¹, and seeded molecular dynamics⁹², FFS represents a "gold standard" approach when dealing with ice nucleation (see e.g. Refs. 35,44,57,89,93). This method involves partitioning the path from (in this case) liquid water to ice, described by an order parameter λ , into a collection of interfaces λ_i . Here, λ corresponds to the number of water molecules within the largest ice nucleus, which can be located either in the bulk of the water slab or at the water-CHLM₀₀₁^{OH} interface. A diffuse crystal-liquid interface has been taken into account into the definition of λ , which relies on local bond order parameters (see SI and Ref. 94), consistent with Ref. 44. Starting from the natural fluctuations of liquid water toward the ice phase, i.e. pre-critical ice nuclei as sampled within μs long unbiased MD simulations, the nucleation rate \mathcal{J} can be obtained as the product of the flux Φ_{λ_0} by which the system reached the first interface λ_0 , times the product of the sequence of the individual crossing probabilities $P(\lambda_i|\lambda_{i-1})$:

$$\mathcal{J} = \Phi_{\lambda_0} \prod_{i=1}^{N_\lambda} P(\lambda_i|\lambda_{i-1}) \quad (2)$$

In this way, the (exceedingly small) total probability $P(\lambda_{ice}|\lambda_0)$ for a certain MD trajectory to reach the ice basin is decomposed in a collection of (manageable) crossing probabilities which we compute by a large number (10^3 to 10^5) of unbiased MD trial runs from λ_{i-1} to λ_i . Further details about the FFS algorithm can be found in the SI. We note that we have used the same water model (TIP4P/Ice) at the same strong supercooling ($\Delta T_S = 42$ K) as employed previously to compute the homogeneous ice nucleation rate and the heterogeneous ice nucleation rate on kaolinite, a clay mineral of relevance to atmospheric science. As such, we can compare directly our results with those of Refs. 57 and 44.

From the very early stages of the nucleation process, we observe a strong preference for ice to form at the water-CHLM₀₀₁^{OH} interface - as opposed to within the bulk of the water slab. In fact, $\sim 75\%$ of the pre-critical ice nuclei we observe as natural fluctuations of the supercooled water network ($\lambda=0$) sit on top of the CHLM₀₀₁^{OH} surface. The calculated growth probability $P(\lambda|\lambda_0)$ as a function of lambda, together with the fraction of ice nuclei that can be found at the water-CHLM₀₀₁^{OH} interface are reported in the SI (Fig. S2b). By the time the FFS algorithm has reached $\lambda=125$, no nuclei within the bulk of the water slab survive. We have observed a similar trend in the case of ice nucleation on the hydroxylated (001) basal face of kaolinite⁴⁴, but the fraction of ice nuclei at the water-kaolinite interface at the initial stages of the FFS algorithm was much smaller ($\sim 25\%$). This suggests that pre-critical ice-like fluctuations, which we have recently investigated in the broader context of heterogeneous crystal nucleation⁹⁵, are much more likely to occur at the surface of CHLM compared to kaolinite.

The mechanism of ice nucleation at the water-CHLM₀₀₁^{OH} interface is illustrated in Fig. 5: the early stages involve the formation of elongated, almost one dimensional, linear, chain-like ice nuclei preferentially

along specific directions (see SI), due to the particular arrangement of the -OH hydroxyl groups on the $\text{CHLM}_{001}^{-\text{OH}}$ surface. However, larger nuclei (corresponding to increasing values of λ) progressively assume a more isotropic shape, as indicated by the evolution of the asphericity parameter α (equal to 1 and 0 for a infinitely elongated rod and a perfect sphere respectively) as a function of λ . At the same time, the 1D character of the nuclei evolves toward a more compact geometry, with a significant growth along the [001] direction (z-axis) normal to the water- $\text{CHLM}_{001}^{-\text{OH}}$ interface, as demonstrated by the trend of the dimension ΔZ of the ice nuclei along that axis, also reported in Fig. 5. The resulting morphology of the ice crystals, though, remains to be investigated because of the emergence of finite size effects. Overall, the evolution of the ice nuclei within the early stage of ice nucleation at the water- $\text{CHLM}_{001}^{-\text{OH}}$ interface possesses some similarities with the case of ice formation on kaolinite⁴⁴, where ice nuclei spread into a 2D, planar geometry before stacking additional ice layers along the normal to the water-kaolinite interface, once the critical nucleus has been reached. Thus, these findings suggest that the nature of the early stages of heterogeneous ice nucleation at strong supercooling ($\Delta T_S = 42$ K) has a strong anisotropic character, in stark contrast with the assumptions prescribed by classical nucleation theory (CNT)⁹⁶.

In fact, CNT does not take into account the molecular structure nor the "chemistry" of the substrate: these aspects are only implicitly included into the value of the contact angle of the ice nuclei with respect to the substrate. However, microscopic features such as the particular arrangement of the hydroxyl groups on the CHLM surface can influence the shape and the energetics of the ice nuclei. In the case of ice on CHLM, water molecules at the water-cholesterol interface find convenient to harness the directionality of the -OH pattern (see Fig. 3a and Fig. 3 in the SI) to form anisotropic ice nuclei (see Fig. 5 and Fig. 3 in the SI), which are likely to be characterised by a much smaller interfacial energy if compared to the hemispherical shape predicated by CNT in the case of perfectly flat, featureless substrates. We note however that in order to probe this aspect of CNT quantitatively, it would be desirable to improve the current enhanced sampling techniques to take into account milder supercooling - and thus larger critical ice nuclei.

The ice nucleation rate on the $\text{CHLM}_{001}^{-\text{OH}}$ surface obtained from our FFS simulations is $10^{27 \pm 3} \text{ s}^{-1} \text{ m}^{-3}$, about 20 orders of magnitude larger than the homogeneous ice nucleation rate at the same supercooling - calculated via FFS simulations using the same water model⁵⁷. This spectacular enhancement of the kinetics of ice formation is due to the small heterogeneous critical nucleus size N_H^* , which we estimate (as discussed in detail in the SI) to contain 250 ± 50 water molecules - a number consistent with the predictions of CNT (see SI and Ref. 44). Interestingly, these results are very similar to what we have previously obtained in the case of ice formation on kaolinite⁴⁴, where we calculated $\mathcal{J} = 10^{26 \pm 2} \text{ s}^{-1} \text{ m}^{-3}$ and $N_H^* = 225 \pm 25$. However, it has to be said that the FFS simulations performed in this work (as opposed to the case of kaolinite⁴⁴) may be suffering from finite size ef-

fects (discussed in the SI), which could both enhance the kinetics of ice nucleation (as the ice nuclei feel the influence of their periodic images) and/or hamper the growth of ice crystals (as the simulation box most likely does not match the periodicity of the growing ice crystal). Our estimates of \mathcal{J} and N_H^* have therefore to be taken with care.

The fact that the kinetics of ice formation on the $\text{CHLM}_{001}^{-\text{OH}}$ surface seems to be comparable with that of an inorganic crystal such as kaolinite is not entirely unexpected, as the (001) hydroxylated surface of kaolinite also presents -OH groups at the water-crystal interface which are capable of templating the formation of ice-like structures. However, supercooled water on kaolinite forms a dense, hexagonal ordered overlayer of ice-like molecules sitting on top of the hydroxyl groups⁴⁵, while, as we have discussed in the previous section, water molecules can partially infiltrate the $\text{CHLM}_{001}^{-\text{OH}}$ surface to form 5- and 6- membered hydrogen bonded rings, resulting in a much less ordered and way less dense overlayer. As both substrates (kaolinite and CHLM) are characterised by the presence of hydroxyl groups which facilitate the formation of ice, the much faster kinetics of ice nucleation we have observed experimentally for CHLM compared to kaolinite (especially at mild supercooling, Fig. 1b) is likely to be due to the different surface topography of the two compounds.

E. Competition between cubic and hexagonal ice

At the strong supercooling considered here ($\Delta T_S = 42$ K), homogeneous ice nucleation results in a mixture of ice I_c and ice I_h known as stacking disordered ice I_{sd} ⁹⁷⁻⁹⁹. However, things can be quite different in the heterogeneous case. For instance, the hydroxylated (001) basal face of kaolinite promotes exclusively the formation of the primary prism face of ice I_h ^{44,45}. In the case of the $\text{CHLM}_{001}^{-\text{OH}}$ surface, we observe both ice I_c and ice I_h nuclei at the very early stages of the nucleation process, as depicted in the inset (left side) of Fig. 6. These ice-like fluctuations originate from the templating effect of the hydroxyl groups on the CHLM surface, as illustrated in Fig. 4a-e (and Fig.S3 in the SI). In principle, even if ice I_c nuclei are three times more abundant than ice I_h nuclei at the first FFS interface ($\lambda = 80$), we would expect the formation of ice on the $\text{CHLM}_{001}^{-\text{OH}}$ surface to proceed via the growth of ice I_{sd} . In fact, as shown in Fig. 6, the competition between the growth of two ice polytypes at 230 K (i.e. $\Delta T = 42$ K) is dominated by ice I_c : by the time the ice nuclei have reached a post-critical size (e.g. $\lambda = 360$), the average number of Hexagonal Cages (HC⁵⁷, the building blocks of ice I_h) is still about three times larger than that of DDC (Double Diamond Cages⁵⁷, the building blocks of ice I_c).

Interestingly, despite the predominance of ice I_c within the growing ice nuclei, ice I_h can still form and grow along a specific direction (the [111] of the cubic phase) on top of ice I_c crystals (which in turn grow along the [100] direction, normal to the plane of the water- $\text{CHLM}_{001}^{-\text{OH}}$ interface), as illustrated in the insets (right side) of Fig. 6.

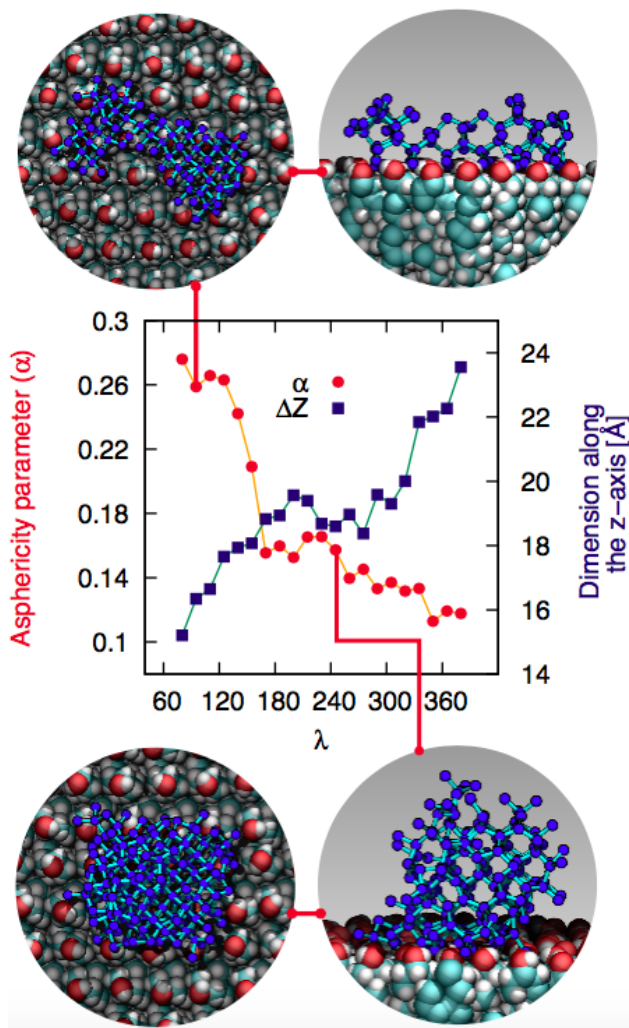


FIG. 5. The early stages of ice nucleation at the water- $\text{CHLM}_{001}^{-\text{OH}}$ interface involve non-spherical ice crystallites. Asphericity parameter α and spatial extent of the ice nuclei along the direction normal to the CHLM slab ΔZ as a function of λ for ice nuclei at the water- $\text{CHLM}_{001}^{-\text{OH}}$ interface. The insets correspond to top and side views of typical ice nuclei forming at the water- $\text{CHLM}_{001}^{-\text{OH}}$ interface, containing about 100 (top) and 245 (bottom) water molecules.

The coexistence of ice I_c and ice I_h is thus likely to result in ice I_{sd} crystals at strong supercooling. However, at milder supercooling ice I_h fluctuations are expected to become more relevant, and in fact experimental evidence suggests that the macroscopic crystalline habit of ice crystals grown on CHLM at $\Delta T=2$ K is indeed that of ice I_h ²². Importantly, we did not observe such a competition between ice I_c and ice I_h in the case of kaolinite, where the cubic polytype is basically absent throughout the whole nucleation process^{44,45}. In fact, we argue that, in the case of CHLM crystals, different nucleation sites (whose exact nature remains to be determined) could promote chiefly ice I_c or ice I_h according to the different degree of supercooling, thus contributing to unravel the strong ice nucleating ability of CHLM crystals along such a wide range of temperatures. This argument would suggest that the multi-component nature of ice nucleation on biological matter could be at least par-

tially attributed to a greater variety of nucleation sites – as well as the specific templating effect of functional groups acting as hydrogen bond donor and/or acceptors with respect to supercooled liquid water. Moreover, we have shown in this work that some of these functional groups – such as the hydroxyl groups characterising the water- $\text{CHLM}_{001}^{-\text{OH}}$ interface – can even promote a different ice polytype at the same time, possibly according to different supercooling.

Finally, we note that, in agreement with previous simulations of ice nucleation^{43,45}, the flexibility of the $\text{CHLM}_{001}^{-\text{OH}}$ has an impact on the extent and the structure of the ice-like fluctuations at the $\text{CHLM}_{001}^{-\text{OH}}$ -water interface, and that the anhydrous crystalline phase of CHL also displays substantial ice nucleating potential. These two aspects are both addressed in detail in the SI.

IV. CONCLUSIONS

By means of a blend of experiments and simulations, we have unravelled the the origins of ice nucleation on cholesterol (CHL), a prototypical organic crystal of relevance to cryopreservation. Our results suggest that its exceptional ice nucleating activity stems from the ability of its flexible hydrophilic surface to form unconventional ice-templating structures – specifically, hydrogen bonded cages comprising 6- as well as 5-membered rings. In addition, the experimental evidence reported here suggests that the intrinsic potential of cholesterol to nucleate ice may potentially be enhanced by specific topological features of the crystalline habit. In particular, droplet freezing measurements show that cholesterol promotes the heterogeneous formation of ice across a wide range of temperatures (from -4 to -20 °C). In fact, we find that CHLM crystals nucleate ice far better than the mineral feldspar, which is one of the most effective inorganic ice nucleating agents of relevance to atmospheric science. Moreover, electron microscopy measurements suggest that the broad range of freezing temperatures we observe for CHLM crystals may be due to the coexistence of diverse structural features of the crystalline surface, which in turn can act as different nucleation sites. The microscopic structure of the latter remains to be assessed, but the possibility that different parts of the CHLM surface may nucleate ice with different efficiency suggests that surface topography can play an important role in determining the ice nucleating ability of organic crystals.

Surprisingly, we find that CHLM crystals, despite being exceptionally good ice nucleating agents, do not provide a conventional template for ice to form. Specifically, molecular simulations reveal that, as opposed to what has been reported for supercooled water in contact with simple model substrates (e.g. Lennard-Jones crystals, which allow to rapidly explore different surface geometries⁷⁸) and/or inorganic materials (such as carbonaceous particles⁴², or clay minerals^{44,45}), water on the (001) hydroxylated surface of cholesterol monohydrate (the most abundant interface in aqueous environments) does not form an ordered, dense, ice-like overlayer. In-

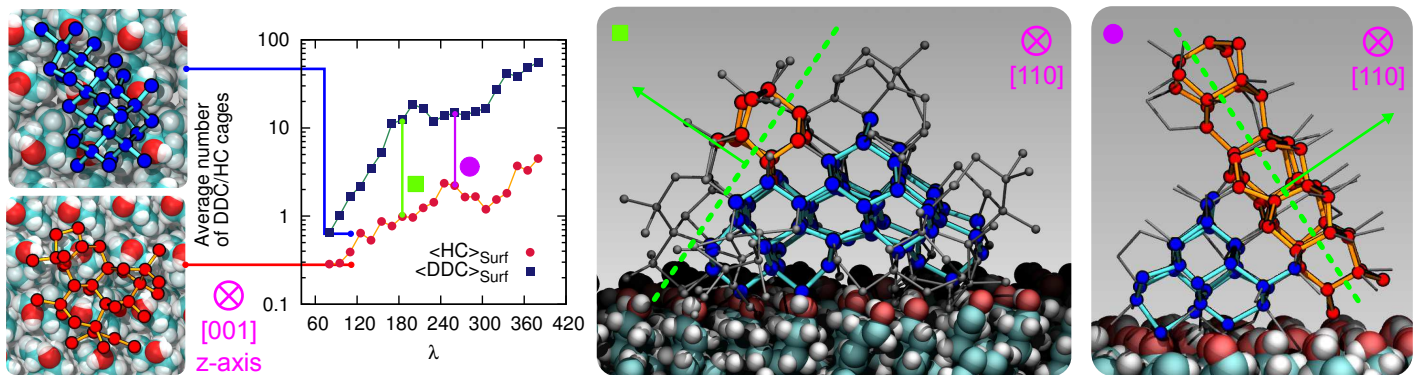


FIG. 6. Competition between cubic (blue/cyan spheres/sticks) and hexagonal (red/orange spheres/sticks) ice within the early stage of ice nucleation at the water- $\text{CHLM}_{001}^{\text{OH}}$ interface. The average number of double diamond and hexagonal cages (DDC and HC, the building block of ice I_c and ice I_h respectively) is reported as a function of the order parameter λ . Insets on the left show representative ice I_c and ice I_h fluctuations (top view) at the first FFS interface ($\lambda=80$). Insets on the right show representative ice nuclei at $\lambda=165$ and 260 , where the competition between the two polymorphs becomes more evident. The dashed (green) lines/arrows indicate the crystallographic plane/direction along with ice I_h has the possibility to grow on top of ice I_c .

stead, due to the flexibility of the CHLM surface and its relatively low density of hydroxyl groups, water molecules partially infiltrate the crystal, forming a network of both 6- and 5-membered hydrogen bonded rings. The latter involve water molecules as well as hydroxyl groups provided by CHL molecules. While some of these structural features (particularly pentagonal rings) are known to hinder homogeneous water freezing, we find that they actually facilitate the heterogeneous formation of both hexagonal and cubic ice on CHLM crystals. In fact, enhanced sampling simulations suggest the emergence of stacking disordered ice (a mixture of the two polytypes) at the water-CHLM interface. This is in stark contrast with what we have previously observed in the case of e.g. the clay mineral kaolinite, where only the hexagonal polytype was observed along the whole nucleation process⁴⁴. In fact, more often than not a given crystalline substrate nucleates exclusively one of the two ice polytypes^{7,13}. Moreover, we find that the nucleation rate of ice on CHLM crystals is basically identical to that we have previously calculated in the case of kaolinite - at the same strong supercooling ($\Delta T_S = 42$ K). Kaolinite and CHLM are both characterised by a hydrogen bond network capable of facilitating the formation of ice nuclei: thus, the substantial difference in the ice nucleating ability we observe experimentally for these two compounds is most likely rooted into their surface topography. In fact, the n_s data reported in Fig. 1b suggest that two populations of potentially different ice nucleating sites may coexist on the CHLM surface. The change in the slope of the CHLM data is reminiscent of that observed for freezing spectra for birch pollen^{17,100}, which has been attributed to the presence of two different ice nucleating macromolecules¹⁰¹. Similarly, we argue that there may be two different broad classes of ice nucleating sites on CHLM, represented by the two different slopes in the freezing spectra. Due to the spatially sporadic nature of the highly active sites, which are not present in every millimetre diameter droplet, it seems likely that these two different classes of ice nucleation sites are related to

specific defects or the diverse topography of the CHLM, rather than any factors related to the bulk molecular structure of CHLM.

In addition, the emergence of stacking disordered ice phases during the heterogeneous formation of ice has been experimentally observed⁹⁹, and consequently ascribed to different crystal growth regimes. Our results offer the intriguing prospect that the nucleation process itself may favour, in some cases, the formation of stacking disordered ices. Thus, we argue that the dramatic ice nucleation ability of certain organic materials may be traced down not only to the formation of a network of hydrogen bonds between water and the nucleation sites, but also to the capability of specific surfaces to promote at the same time different ice polytypes as a function of supercooling. In order to verify this hypothesis, though, we would need to investigate ice nucleation on CHLM at milder supercooling. To this end, an heterogeneous seeded molecular dynamics approach is currently being validated¹⁰². Our results also suggest that organic crystals sit in between inorganic and biological materials, when it comes to promoting the formation of ice: substrates like CHLM are characterised by relatively flat surfaces exposing an array of amphoteric functional groups, much like several inorganic ice nucleating agents (e.g. kaolinite, feldspar, hydroxylated graphene), but the flexibility of the surface and the low density of such functional groups is typical of biological nucleating agents such as macromolecules and bacterial fragments. This is especially relevant in the case of CHL, a molecule which is not only used in crystalline form as an ice nucleating agent in cryopreservation applications, but that significantly contributes to the composition of animal cell membranes as well.

In summary, the experiments and simulations presented in this work indicate that cholesterol crystals are incredibly efficient ice nucleating agents, active across a broad range of supercooling. We show that such strong ice nucleating activity is due to the intrinsic potential of the flexible amphoteric surfaces of CHLM to form unconventional ice-templating molecular structures. It is likely

that microscopic structural features of the crystals could further enhance the ability of CHLM (and potentially of other organic crystals) to form ice, by offering a diverse array of nucleating sites. In fact, we believe that for an ice nucleating agent to be very efficient, a combination of interfacial “chemistry” and surface topography is generally required. This interplay could thus be the key to understand the heterogeneous formation of ice on molecular organic crystals, and it may provide a starting point for the investigation of ice in soft and biological matter at the molecular level. In particular, tailoring the microscopic structure of the substrate and modifying the nature as well as the density of hydrogen-bonding functional groups at the water-substrate interface can be seen as two different routes to engineer the ice nucleating ability of novel cryoprotectants, the design of which, at the moment, largely relies on the high-throughput screening of whole libraries of different compounds. The absence of a proper structure-to-function paradigm is perhaps the most pressing challenge in cryobiology: this is why future work will be devoted to assess whether and how hydrogen-bonding functional groups other than hydroxyls would be equally effective to enhance the kinetics of heterogeneous ice nucleation.

CONFLICTS OF INTEREST

There are no conflicts to declare.

ACKNOWLEDGEMENTS

This work was supported by the European Research Council (ERC) under the European Union’s Seventh Framework Programme: Grant Agreement number 616121 (HeteroIce project [AM, PP, GCS]), Grant Agreement number 632272 (IceControl project [TFW, BJM]) and Grant Agreement number 648661 (MarineIce project [TFW, BJM]). MAH and BJM are also supported by the Engineering Physical Sciences Research Council (EPSRC) via the Research Grant number EP/M003027/1. GCS and PP acknowledge the use of the UCL Grace and Legion High Performance Computing Facilities, the use of Emerald, a GPU-accelerated High Performance Computer, made available by the Science & Engineering South Consortium operated in partnership with the STFC Rutherford-Appleton Laboratory and the use of ARCHER UK National Supercomputing Service (<http://www.archer.ac.uk>) through the Materials Chemistry Consortium via the EPSRC grant number EP/L000202. The Forward Flux Sampling simulations were supported by a grant from the Swiss National Supercomputing Centre (CSCS; project ID s758).

SUPPLEMENTARY INFORMATION

Supplementary Information (SI) can be found at:

<http://www.rsc.org/suppdata/c8/sc/c8sc02753f/c8sc02753f1.pdf>

- ¹Thorsten Bartels-Rausch. Chemistry: Ten things we need to know about ice and snow. *Nature*, 494(7435):27–29, February 2013. ISSN 0028-0836. doi:10.1038/494027a. URL <http://www.nature.com/nature/journal/v494/n7435/full/494027a.html>.
- ²E Mocé, E Blanch, C Tomás, and Jk Graham. Use of Cholesterol in Sperm Cryopreservation: Present Moment and Perspectives to Future. *Reprod. Domest. Anim.*, 45: 57–66, June 2010. ISSN 1439-0531. doi:10.1111/j.1439-0531.2010.01635.x. URL <http://onlinelibrary.wiley.com/doi/10.1111/j.1439-0531.2010.01635.x/abstract>.
- ³Isobel Massie, Clare Selden, Humphrey Hodgson, Barry Fuller, Stephanie Gibbons, and G. John Morris. GMP Cryopreservation of Large Volumes of Cells for Regenerative Medicine: Active Control of the Freezing Process. *Tissue Eng. Part C Methods*, 20(9):693–702, January 2014. ISSN 1937-3384. doi:10.1089/ten.tec.2013.0571. URL <http://online.liebertpub.com/doi/full/10.1089/ten.tec.2013.0571>.
- ⁴John Morris and Elizabeth Acton. Controlled ice nucleation in cryopreservation A review. *Cryobiology*, 66(2):85–92, April 2013. ISSN 0011-2240. doi:10.1016/j.cryobiol.2012.11.007. URL <http://www.sciencedirect.com/science/article/pii/S0011224012002660>.
- ⁵B. J. Murray, D. O’Sullivan, J. D. Atkinson, and M. E. Webb. Ice nucleation by particles immersed in supercooled cloud droplets. *Chem. Soc. Rev.*, 41(19):6519–6554, September 2012. ISSN 1460-4744. doi:10.1039/C2CS35200A. URL <http://pubs.rsc.org/en/content/articlelanding/2012/cs/c2cs35200a>.
- ⁶Ben Slater, Angelos Michaelides, Christoph G. Salzmann, and Ulrike Lohmann. A Blue-Sky Approach to Understanding Cloud Formation. *Bull. Amer. Meteor. Soc.*, 97(10):1797–1802, December 2015. ISSN 0003-0007. doi:10.1175/BAMS-D-15-00131.1. URL <http://journals.ametsoc.org/doi/abs/10.1175/BAMS-D-15-00131.1>.
- ⁷Gabriele C. Sossio, Ji Chen, Stephen J. Cox, Martin Fitzner, Philipp Pedevilla, Andrea Zen, and Angelos Michaelides. Crystal Nucleation in Liquids: Open Questions and Future Challenges in Molecular Dynamics Simulations. *Chem. Rev.*, 116(12):7078–7116, June 2016. ISSN 0009-2665. doi:10.1021/acs.chemrev.5b00744. URL <http://dx.doi.org/10.1021/acs.chemrev.5b00744>.
- ⁸U. Lohmann and J. Feichter. Global indirect aerosol effects: a review. *Atmos. Chem. Phys.*, 5(3):715–737, March 2005. ISSN 1680-7324. doi:10.5194/acp-5-715-2005. URL <http://www.atmos-chem-phys.net/5/715/2005/>.
- ⁹Ivy Tan, Trude Storelvmo, and Mark D. Zelinka. Observational constraints on mixed-phase clouds imply higher climate sensitivity. *Science*, 352(6282):224–227, April 2016. ISSN 0036-8075, 1095-9203. doi:10.1126/science.aad5300. URL <http://science.sciencemag.org/content/352/6282/224>.
- ¹⁰C. Marcolli, B. Nagare, A. Welti, and U. Lohmann. Ice nucleation efficiency of AgI: review and new insights. *Atmos. Chem. Phys.*, 16(14):8915–8937, July 2016. ISSN 1680-7324. doi:10.5194/acp-16-8915-2016. URL <http://www.atmos-chem-phys.net/16/8915/2016/>.
- ¹¹James D. Atkinson, Benjamin J. Murray, Matthew T. Woodhouse, Thomas F. Whale, Kelly J. Baustian, Kenneth S. Carslaw, Steven Dobbie, Daniel O’Sullivan, and Tamsin L. Malkin. The importance of feldspar for ice nucleation by mineral dust in mixed-phase clouds. *Nature*, 498(7454):355–358, June 2013. ISSN 0028-0836. doi:10.1038/nature12278. URL <https://www.nature.com/nature/journal/v498/n7454/full/nature12278.html>.
- ¹²A. D. Harrison, T. F. Whale, M. A. Carpenter, M. A. Holden, L. Neve, D. O’Sullivan, J. Vergara Temprado, and B. J. Murray. Not all feldspars are equal: a survey of ice nucleating properties across the feldspar group of minerals. *Atmos. Chem. Phys.*, 16(17):10927–10940, September 2016. ISSN 1680-7324. doi:10.5194/acp-16-10927-2016. URL <http://www.atmos-chem-phys.net/16/10927/2016/>.
- ¹³Alexei Kiselev, Felix Bachmann, Philipp Pedevilla, Stephen J. Cox, Angelos Michaelides, Dagmar Gerthsen, and Thomas Leisner. Active sites in heterogeneous ice nucleation: the example of K-rich feldspars. *Science*, 355(6323):367–371, January 2017. ISSN 0036-8075, 1095-9203. doi:10.1126/science.aai8034. URL

- <http://science.sciencemag.org/content/355/6323/367>.
- ¹⁴Leroy R. Maki, Elizabeth L. Galyan, Mei-Mon Chang-Chien, and Daniel R. Caldwell. Ice Nucleation Induced by *Pseudomonas syringae*1. *Appl. Microbiol.*, 28(3):456–459, September 1974. ISSN 0003-6919. URL <http://www.ncbi.nlm.nih.gov/pmc/articles/PMC186742/>.
 - ¹⁵Julianne Lindemann, Gareth J. Warren, and Trevor V. Suslow. Ice-Nucleating Bacteria. *Science*, 231(4738): 536–536, February 1986. ISSN 0036-8075, 1095-9203. doi:10.1126/science.231.4738.536-c. URL <http://science.sciencemag.org/content/231/4738/536.4>.
 - ¹⁶Ravindra Pandey, Kota Usui, Ruth A. Livingstone, Sean A. Fischer, Jim Pfaendtner, Ellen H. G. Backus, Yuki Nagata, Janine Fröhlich-Nowoisky, Lars Schmöser, Sergio Mauri, Jan F. Scheel, Daniel A. Knopf, Ulrich Pöschl, Mischa Bonn, and Tobias Weidner. Ice-nucleating bacteria control the order and dynamics of interfacial water. *Sci. Adv.*, 2(4):e1501630, April 2016. ISSN 2375-2548. doi:10.1126/sciadv.1501630. URL <http://advances.sciencemag.org/content/2/4/e1501630>.
 - ¹⁷B. G. Pummer, H. Bauer, J. Bernardi, S. Bleicher, and H. Grothe. Suspendable macromolecules are responsible for ice nucleation activity of birch and conifer pollen. *Atmos. Chem. Phys.*, 12(5):2541–2550, March 2012. ISSN 1680-7324. doi:10.5194/acp-12-2541-2012. URL <http://www.atmos-chem-phys.net/12/2541/2012/>.
 - ¹⁸Maya Bar Dolev, Ido Braslavsky, and Peter L. Davies. Ice-Binding Proteins and Their Function. *Annu. Rev. Biochem.*, 85(1):515–542, June 2016. ISSN 0066-4154. doi:10.1146/annurev-biochem-060815-014546. URL <https://0-www-annualreviews-org.pugwash.lib.warwick.ac.uk/doi/10.1146/annurev-biochem-060815-014546>.
 - ¹⁹Waseem Asghar, Rami El Assal, Hadi Shafiee, Raymond M. Anchan, and Utkan Demirci. Preserving human cells for regenerative, reproductive, and transfusion medicine. *Biotechnol. J.*, 9(7):895–903, July 2014. ISSN 1860-6768. doi:10.1002/biot.201300074. URL <https://www.ncbi.nlm.nih.gov/pmc/articles/PMC4145864/>.
 - ²⁰Ayesha Aijaz, Matthew Li, David Smith, Danika Khong, Courtney LeBlon, Owen S. Fenton, Ronke M. Olabisi, Steven Libutti, Jay Tischfield, Marcela V. Maus, Robert Deans, Rita N. Barcia, Daniel G. Anderson, Jerome Ritz, Robert Preti, and Biju Parekkadan. Biomanufacturing for clinically advanced cell therapies. *Nat. Biomed. Eng.*, 2(6):362–376, June 2018. ISSN 2157-846X. doi:10.1038/s41551-018-0246-6. URL <http://0-www-nature-com/articles/s41551-018-0246-6>.
 - ²¹N Fukuta and B. J. Mason. Epitaxial growth of ice on organic crystals. *J. Phys. Chem. Sol.*, 24(6):715–718, June 1963. ISSN 0022-3697. doi:10.1016/0022-3697(63)90217-8. URL <http://www.sciencedirect.com/science/article/pii/0022369763902178>.
 - ²²N. Fukuta. Experimental Studies of Organic Ice Nuclei. *J. Atmos. Sci.*, 23(2):191–196, March 1966. ISSN 0022-4928. doi:10.1175/1520-0469(1966)023<0191:ESOOIN>2.0.CO;2. URL <http://journals.ametsoc.org/doi/abs/10.1175/1520-0469%281966%29023%3C0191%3AESOOIN%3E2.0.CO%3B2>.
 - ²³Richard B. Head. Steroids as Ice Nucleators. *Nature*, 191(4793):1058–1059, September 1961. doi:10.1038/1911058a0. URL <http://www.nature.com.libproxy.ucl.ac.uk/nature/journal/v191/n4793/abs/1911058a0.html>.
 - ²⁴Isobel Massie, Clare Selden, Humphrey Hodgson, and Barry Fuller. Cryopreservation of Encapsulated Liver Spheroids for a Bioartificial Liver: Reducing Latent Cryoinjury Using an Ice Nucleating Agent. *Tissue Eng. Part C Methods*, 17(7):765–774, July 2011. ISSN 1937-3384, 1937-3392. doi:10.1089/ten.tec.2010.0394. URL <http://www.liebertonline.com/doi/abs/10.1089/ten.tec.2010.0394>.
 - ²⁵Martin R. Krause and Steven L. Regen. The Structural Role of Cholesterol in Cell Membranes: From Condensed Bilayers to Lipid Rafts. *Acc. Chem. Res.*, 47(12):3512–3521, December 2014. ISSN 0001-4842, 1520-4898. doi:10.1021/ar500260t. URL <http://pubs.acs.org/doi/10.1021/ar500260t>.
 - ²⁶G. R. Edwards and L. F. Evans. The Mechanism of Activation of Ice Nuclei. *J. Atmos. Sci.*, 28(8): 1443–1447, November 1971. ISSN 0022-4928. doi:10.1175/1520-0469(1971)028<1443:TMOAOI>2.0.CO;2. URL <http://journals.ametsoc.org/doi/abs/10.1175/1520-0469%281971%29028%3C1443%3ATMOAOI%3E2.0.CO%3B2>.
 - ²⁷Kerri A. Pratt, Paul J. DeMott, Jeffrey R. French, Zhihen Wang, Douglas L. Westphal, Andrew J. Heymsfield, Cynthia H. Twohy, Anthony J. Prenni, and Kimberly A. Prather. In situ detection of biological particles in cloud ice-crystals. *Nature Geosci.*, 2(6):398–401, June 2009. ISSN 1752-0894. doi:10.1038/ngeo521. URL <http://www.nature.com/ngeo/journal/v2/n6/full/ngeo521.html>.
 - ²⁸C. Hoese, J. E. Kristjánsson, and S. M. Burrows. How important is biological ice nucleation in clouds on a global scale? *Environ. Res. Lett.*, 5(2):024009, 2010. ISSN 1748-9326. doi:10.1088/1748-9326/5/2/024009. URL <http://stacks.iop.org/1748-9326/5/i=2/a=024009>.
 - ²⁹Bingbing Wang, Andrew T. Lambe, Paola Massoli, Timothy B. Onasch, Paul Davidovits, Douglas R. Worsnop, and Daniel A. Knopf. The deposition ice nucleation and immersion freezing potential of amorphous secondary organic aerosol: Pathways for ice and mixed-phase cloud formation. *J. Geophys. Res.*, 117(D16):D16209, August 2012. ISSN 2156-2202. doi:10.1029/2012JD018063. URL <http://onlinelibrary.wiley.com/doi/10.1029/2012JD018063/abstract>.
 - ³⁰Peter L. Davies. Ice-binding proteins: a remarkable diversity of structures for stopping and starting ice growth. *Trends Biochem. Sci.*, 39(11):548–555, November 2014. ISSN 0968-0004. doi:10.1016/j.tibs.2014.09.005. URL <http://www.sciencedirect.com/science/article/pii/S0968000414001716>.
 - ³¹Kai Liu, Chunlei Wang, Ji Ma, Guosheng Shi, Xi Yao, Haiping Fang, Yanlin Song, and Jianjun Wang. Janus effect of antifreeze proteins on ice nucleation. *Proc. Natl. Acad. Sci. U.S.A.*, 113(51):14739–14744, December 2016. ISSN 0027-8424, 1091-6490. doi:10.1073/pnas.1614379114. URL <http://www.pnas.org/content/113/51/14739>.
 - ³²James M. Campbell, Fiona C. Meldrum, and Hugo K. Christenson. Observing the formation of ice and organic crystals in active sites. *Proc. Natl. Acad. Sci. U.S.A.*, 114(5):810–815, January 2017. ISSN 0027-8424, 1091-6490. doi:10.1073/pnas.1617717114. URL <http://www.pnas.org/content/114/5/810>.
 - ³³Stephen A. Zielke, Allan K. Bertram, and G. N. Patey. Simulations of Ice Nucleation by Kaolinite (001) with Rigid and Flexible Surfaces. *J. Phys. Chem. B*, 120(8):1726–1734, March 2016. ISSN 1520-6106. doi:10.1021/acs.jpcc.5b09052. URL <http://dx.doi.org/10.1021/acs.jpcc.5b09052>.
 - ³⁴Xiang-Xiong Zhang, Min Chen, and Ming Fu. Impact of surface nanostructure on ice nucleation. *J. Chem. Phys.*, 141(12): 124709, 2014. URL <http://scitation.aip.org/content/aip/journal/jcp/141/12/10.1063/1.4896149>.
 - ³⁵Yuanfei Bi, Raffaella Cabriolu, and Tianshu Li. Heterogeneous Ice Nucleation Controlled by the Coupling of Surface Crystallinity and Surface Hydrophilicity. *J. Phys. Chem. C*, 120(3):1507–1514, January 2016. ISSN 1932-7447. doi:10.1021/acs.jpcc.5b09740. URL <http://dx.doi.org/10.1021/acs.jpcc.5b09740>.
 - ³⁶Aleks Reinhardt and Jonathan P. K. Doye. Effects of surface interactions on heterogeneous ice nucleation for a monatomic water model. *J. Chem. Phys.*, 141(8): 084501, August 2014. ISSN 0021-9606, 1089-7690. doi:10.1063/1.4892804. URL <http://scitation.aip.org/content/aip/journal/jcp/141/8/10.1063/1.4892804>.
 - ³⁷Guillaume Fraux and Jonathan P. K. Doye. Note: Heterogeneous ice nucleation on silver-iodide-like surfaces. *J. Chem. Phys.*, 141(21):216101, December 2014. ISSN 0021-9606, 1089-7690. doi:10.1063/1.4902382. URL <http://scitation.aip.org/content/aip/journal/jcp/141/21/10.1063/1.4902382>.
 - ³⁸Philipp Pedevilla, Martin Fitzner, and Angelos Michaelides. What makes a good descriptor for heterogeneous ice nucleation on OH-patterned surfaces. *Phys. Rev. B*, 96(11):115441, September 2017. doi:10.1103/PhysRevB.96.115441. URL <https://link.aps.org/doi/10.1103/PhysRevB.96.115441>.
 - ³⁹Laura Lupi, Rebecca Hanscam, Yuqing Qiu, and Valeria Molinero. Reaction Coordinate for Ice Crystallization on a Soft Surface. *J. Phys. Chem. Lett.*, 8(17):4201–4205, September

2017. ISSN 1948-7185. doi:10.1021/acs.jpcllett.7b01855. URL <http://dx.doi.org/10.1021/acs.jpcllett.7b01855>.
- ⁴⁰Yuanfei Bi, Boxiao Cao, and Tianshu Li. Enhanced heterogeneous ice nucleation by special surface geometry. *Nat. Commun.*, 8:15372, May 2017. ISSN 2041-1723. doi:10.1038/ncomms15372. URL <http://www.nature.com/ncomms/2017/170517/ncomms15372/full/ncomms15372.html>.
- ⁴¹Valeria Molinero and Emily B. Moore. Water Modeled As an Intermediate Element between Carbon and Silicon. *J. Phys. Chem. B*, 113(13):4008–4016, April 2009. ISSN 1520-6106. doi:10.1021/jp805227c. URL <http://dx.doi.org/10.1021/jp805227c>.
- ⁴²Laura Lupi, Arpa Hudait, and Valeria Molinero. Heterogeneous Nucleation of Ice on Carbon Surfaces. *J. Am. Chem. Soc.*, 136(8):3156–3164, February 2014. ISSN 0002-7863. doi:10.1021/ja411507a. URL <http://dx.doi.org/10.1021/ja411507a>.
- ⁴³Yueqing Qiu, Nathan Odendahl, Arpa Hudait, Ryan Mason, Allan K. Bertram, Francesco Paesani, Paul J. DeMott, and Valeria Molinero. Ice Nucleation Efficiency of Hydroxylated Organic Surfaces Is Controlled by Their Structural Fluctuations and Mismatch to Ice. *J. Am. Chem. Soc.*, 139(8):3052–3064, March 2017. ISSN 0002-7863. doi:10.1021/jacs.6b12210. URL <http://dx.doi.org/10.1021/jacs.6b12210>.
- ⁴⁴Gabriele C. Sossio, Tianshu Li, Davide Donadio, Gareth A. Tribello, and Angelos Michaelides. Microscopic Mechanism and Kinetics of Ice Formation at Complex Interfaces: Zooming in on Kaolinite. *J. Phys. Chem. Lett.*, 7:2350–2355, June 2016. ISSN 1948-7185. doi:10.1021/acs.jpcllett.6b01013. URL <http://dx.doi.org/10.1021/acs.jpcllett.6b01013>.
- ⁴⁵Gabriele C. Sossio, Gareth A. Tribello, Andrea Zen, Philipp Pedevilla, and Angelos Michaelides. Ice formation on kaolinite: Insights from molecular dynamics simulations. *J. Chem. Phys.*, 145(21):211927, December 2016. ISSN 0021-9606, 1089-7690. doi:10.1063/1.4968796. URL <http://scitation.aip.org/content/aip/journal/jcp/145/21/10.1063/1.4968796>.
- ⁴⁶L. F. Evans. Ice Nucleation by Amino Acids. *J. Atmos. Sci.*, 23(6):751–752, November 1966. ISSN 0022-4928. doi:10.1175/1520-0469(1966)023<0751:INBAA>2.0.CO;2. URL [http://journals.ametsoc.org/doi/abs/10.1175/1520-0469\(1966\)023<0751:INBAA>2.0.CO;2](http://journals.ametsoc.org/doi/abs/10.1175/1520-0469(1966)023<0751:INBAA>2.0.CO;2).
- ⁴⁷M. Gavish, J. L. Wang, M. Eisenstein, M. Lahav, and L. Leiserowitz. The Role of Crystal Polarity in α -Amino Acid Crystals for Induced Nucleation of Ice. *Science*, 256:815–818, 1992. URL <http://www.jstor.org/stable/pdf/2877034.pdf>.
- ⁴⁸P. K. Wolber, C. A. Deininger, M. W. Southworth, J. Vandekerckhove, M. van Montagu, and G. J. Warren. Identification and purification of a bacterial ice-nucleation protein. *Proc. Natl. Acad. Sci. U.S.A.*, 83(19):7256–7260, October 1986. ISSN 0027-8424, 1091-6490. URL <http://www.pnas.org/content/83/19/7256>.
- ⁴⁹D. Gurian-Sherman and S. E. Lindow. Bacterial ice nucleation: significance and molecular basis. *FASEB J.*, 7(14):1338–1343, November 1993. ISSN 0892-6638, 1530-6860. URL <http://www.fasebj.org/content/7/14/1338>.
- ⁵⁰T. F. Whale, B. J. Murray, D. O’Sullivan, T. W. Wilson, N. S. Umo, K. J. Baustian, J. D. Atkinson, D. A. Workneh, and G. J. Morris. A technique for quantifying heterogeneous ice nucleation in microlitre supercooled water droplets. *Atmos. Meas. Tech.*, 8(6):2437–2447, June 2015. ISSN 1867-8548. doi:10.5194/amt-8-2437-2015. URL <http://www.atmos-meas-tech.net/8/2437/2015/>.
- ⁵¹Caroline A. Schneider, Wayne S. Rasband, and Kevin W. Elceiri. NIH Image to ImageJ: 25 years of image analysis. *Nat. Methods*, 9:671–675, 2012.
- ⁵²Bryan M. Craven. Crystal structure of cholesterol monohydrate. *Nature*, 260(5553):727–729, April 1976. doi:10.1038/260727a0. URL <http://www.nature.com/libproxy.ucl.ac.uk/nature/journal/v260/n5553/abs/260727a0.html>.
- ⁵³J. L. F. Abascal, E. Sanz, R. García Fernández, and C. Vega. A potential model for the study of ices and amorphous water: TIP4p/Ice. *J. Chem. Phys.*, 122(23):234511, June 2005. ISSN 0021-9606, 1089-7690. doi:10.1063/1.1931662. URL <http://scitation.aip.org/libproxy.ucl.ac.uk/content/aip/journal/jcp/122/23/10.1063/1.1931662>.
- ⁵⁴Richard S. Abandan and Jennifer A. Swift. Surface Characterization of Cholesterol Monohydrate Single Crystals by Chemical Force Microscopy. *Langmuir*, 18(12):4847–4853, June 2002. ISSN 0743-7463. doi:10.1021/la025649r. URL <http://dx.doi.org/10.1021/la025649r>.
- ⁵⁵Pr Bjelkmar, Per Larsson, Michel A. Cuendet, Berk Hess, and Erik Lindahl. Implementation of the CHARMM Force Field in GROMACS: Analysis of Protein Stability Effects from Correction Maps, Virtual Interaction Sites, and Water Models. *J. Chem. Theory Comput.*, 6(2):459–466, February 2010. ISSN 1549-9618. doi:10.1021/ct900549r. URL <http://dx.doi.org/10.1021/ct900549r>.
- ⁵⁶Joseph B. Lim, Brent Rogaski, and Jeffery B. Klauda. Update of the Cholesterol Force Field Parameters in CHARMM. *J. Phys. Chem. B*, 116(1):203–210, January 2012. ISSN 1520-6106. doi:10.1021/jp207925m. URL <http://dx.doi.org/10.1021/jp207925m>.
- ⁵⁷Amir Haji-Akbari and Pablo G. Debenedetti. Direct calculation of ice homogeneous nucleation rate for a molecular model of water. *Proc. Natl. Acad. Sci. U.S.A.*, 112(34):10582–10588, August 2015. ISSN 0027-8424, 1091-6490. doi:10.1073/pnas.1509267112. URL <http://www.pnas.org/content/112/34/10582>.
- ⁵⁸H. A. Lorentz. Ueber die Anwendung des Satzes vom Virial in der kinetischen Theorie der Gase. *Ann. Phys. (Ber.)*, 248(1):127–136, January 1881. ISSN 1521-3889. doi:10.1002/andp.18812480110. URL <http://onlinelibrary.wiley.com/doi/10.1002/andp.18812480110/abstract>.
- ⁵⁹Giovanni Bussi, Davide Donadio, and Michele Parrinello. Canonical sampling through velocity rescaling. *J. Chem. Phys.*, 126(1):014101, January 2007. ISSN 0021-9606, 1089-7690. doi:10.1063/1.2408420. URL <http://scitation.aip.org/content/aip/journal/jcp/126/1/10.1063/1.2408420>.
- ⁶⁰Shuichi Miyamoto and Peter A. Kollman. Settle: An analytical version of the SHAKE and RATTLE algorithm for rigid water models. *J. Comp. Chem.*, 13(8):952–962, October 1992. ISSN 1096-987X. doi:10.1002/jcc.540130805. URL <http://onlinelibrary.wiley.com/doi/10.1002/jcc.540130805/abstract>.
- ⁶¹Berk Hess, Henk Bekker, Herman J. C. Berendsen, and Johannes G. E. M. Fraaije. LINCS: A linear constraint solver for molecular simulations. *J. Comp. Chem.*, 18(12):1463–1472, September 1997. ISSN 1096-987X. doi:10.1002/(SICI)1096-987X(199709)18:12<1463::AID-JCC4>3.0.CO;2-H. URL [http://onlinelibrary.wiley.com/doi/10.1002/\(SICI\)1096-987X\(199709\)18:12<1463::AID-JCC4>3.0.CO;2-H/abstract](http://onlinelibrary.wiley.com/doi/10.1002/(SICI)1096-987X(199709)18:12<1463::AID-JCC4>3.0.CO;2-H/abstract).
- ⁶²R. J. Herbert, B. J. Murray, T. F. Whale, S. J. Dobbie, and J. D. Atkinson. Representing time-dependent freezing behaviour in immersion mode ice nucleation. *Atmos. Chem. Phys.*, 14(16):8501–8520, August 2014. ISSN 1680-7324. doi:10.5194/acp-14-8501-2014. URL <http://www.atmos-chem-phys.net/14/8501/2014/>.
- ⁶³Thomas F. Whale, Martin Rosillo-Lopez, Benjamin J. Murray, and Christoph G. Salzmann. Ice Nucleation Properties of Oxidized Carbon Nanomaterials. *J. Phys. Chem. Lett.*, 6(15):3012–3016, August 2015. ISSN 1948-7185. doi:10.1021/acs.jpcllett.5b01096. URL <http://dx.doi.org/10.1021/acs.jpcllett.5b01096>.
- ⁶⁴H. S. Shieh, L. G. Hoard, and C. E. Nordman. Crystal structure of anhydrous cholesterol. *Nature*, 267(5608):287–289, May 1977. doi:10.1038/267287a0. URL <http://www.nature.com/nature/journal/v267/n5608/abs/267287a0.html>.
- ⁶⁵C. R. Loomis, G. G. Shipley, and D. M. Small. The phase behavior of hydrated cholesterol. *J. Lipid Res.*, 20(4):525–535, May 1979. ISSN 0022-2275, 1539-7262. URL <http://www.jlr.org/content/20/4/525>.
- ⁶⁶N. Garti, L. Karpuj, and S. Sarig. Correlation between crystal habit and the composition of solvated and nonsolvated cholesterol crystals. *J. Lipid Res.*, 22(5):785–791, July 1981. ISSN 0022-2275, 1539-7262. URL <http://www.jlr.org/content/22/5/785>.

- ⁶⁷Hanna Rapaport, Ivan Kuzmenko, Sylvaine Lafont, Kristian Kjaer, Paul B. Howes, Jens Als-Nielsen, Meir Lahav, and Leslie Leiserowitz. Cholesterol Monohydrate Nucleation in Ultrathin Films on Water. *Biophys. J.*, 81(5):2729–2736, November 2001. ISSN 0006-3495. doi:10.1016/S0006-3495(01)75915-2. URL <http://www.sciencedirect.com/science/article/pii/S0006349501759152>.
- ⁶⁸Inna Solomonov, Markus J. Weygand, Kristian Kjaer, Hanna Rapaport, and Leslie Leiserowitz. Trapping Crystal Nucleation of Cholesterol Monohydrate: Relevance to Pathological Crystallization. *Biophys. J.*, 88(3):1809–1817, March 2005. ISSN 0006-3495. doi:10.1529/biophysj.104.044834. URL <http://www.sciencedirect.com/science/article/pii/S00063495050732458>.
- ⁶⁹R. B. Head. Ice nucleation by some cyclic compounds. *J. Phys. Chem. Sol.*, 23(10):1371–1378, October 1962. ISSN 0022-3697. doi:10.1016/0022-3697(62)90190-7. URL <http://www.sciencedirect.com/science/article/pii/0022369762901907>.
- ⁷⁰G. Vali, P. J. DeMott, O. Möhler, and T. F. Whale. Technical Note: A proposal for ice nucleation terminology. *Atmos. Chem. Phys.*, 15(18):10263–10270, September 2015. ISSN 1680-7324. doi:10.5194/acp-15-10263-2015. URL <http://www.atmos-chem-phys.net/15/10263/2015/>.
- ⁷¹G. Vali. Interpretation of freezing nucleation experiments: singular and stochastic; sites and surfaces. *Atmos. Chem. Phys.*, 14(11):5271–5294, June 2014. ISSN 1680-7324. doi:10.5194/acp-14-5271-2014. URL <http://www.atmos-chem-phys.net/14/5271/2014/>.
- ⁷²Hans Pruppacher and James Klett. *Microphysics of clouds and precipitation*. 1997. ISBN 978-0-7923-4211-3. URL http://books.google.de/books?id=kQ18q7wtP6gC&printsec=frontcover&dq=pruppacher+klett&source=bl&ots=ZBrKwKSwc8&sig=oiVrZTYcCUeyDGOpyP3XddyFriY&hl=de&ei=qawATZ04JoSo8QPC36CbCa&sa=X&oi=book_result&ct=result&resnum=4&ved=0CD0Q6AwAw#v=onepage&q&f=false.
- ⁷³G. Vali. Repeatability and randomness in heterogeneous freezing nucleation. *Atmos. Chem. Phys.*, 8(16):5017–5031, August 2008. ISSN 1680-7324. doi:10.5194/acp-8-5017-2008. URL <http://www.atmos-chem-phys.net/8/5017/2008/>.
- ⁷⁴C.W. Gurganus, J.C. Charnawskas, A.B. Kostinski, and R.A. Shaw. Nucleation at the Contact Line Observed on Nanotextured Surfaces. *Phys. Rev. Lett.*, 113(23):235701, December 2014. doi:10.1103/PhysRevLett.113.235701. URL <https://link.aps.org/doi/10.1103/PhysRevLett.113.235701>.
- ⁷⁵Thomas F. Whale, Mark A. Holden, Alexander N. Kulak, Yi-Yeoun Kim, Fiona C. Meldrum, Hugo K. Christenson, and Benjamin J. Murray. The role of phase separation and related topography in the exceptional ice-nucleating ability of alkali feldspars. *Phys. Chem. Chem. Phys.*, 19(46):31186–31193, November 2017. ISSN 1463-9084. doi:10.1039/C7CP04898J. URL <http://pubs.rsc.org/en/content/articlelanding/2017/cp/c7cp04898j>.
- ⁷⁶David Turnbull and Bernard Vonnegut. Nucleation catalysis. *Ind. Eng. Chem.*, 44(6):1292–1298, 1952.
- ⁷⁷Michael F. Harrach and Barbara Drossel. Structure and dynamics of TIP3p, TIP4p, and TIP5p water near smooth and atomistic walls of different hydroaffinity. *J. Chem. Phys.*, 140(17):174501, May 2014. ISSN 0021-9606. doi:10.1063/1.4872239. URL <http://aip.scitation.org/doi/abs/10.1063/1.4872239>.
- ⁷⁸Martin Fitzner, Gabriele C. Sosso, Stephen J. Cox, and Angelos Michaelides. The Many Faces of Heterogeneous Ice Nucleation: Interplay Between Surface Morphology and Hydrophobicity. *J. Am. Chem. Soc.*, 137(42):13658–13669, October 2015. ISSN 0002-7863. doi:10.1021/jacs.5b08748. URL <http://dx.doi.org/10.1021/jacs.5b08748>.
- ⁷⁹Hiroshi Shintani and Hajime Tanaka. Frustration on the way to crystallization in glass. *Nat. Phys.*, 2(3):200–206, March 2006. ISSN 1745-2473. doi:10.1038/nphys235. URL <http://www.nature.com/nphys/journal/v2/n3/abs/nphys235.html>.
- ⁸⁰Philipp Pedevilla, Stephen J. Cox, Ben Slater, and Angelos Michaelides. Can Ice-Like Structures Form on Non-Ice-Like Substrates? The Example of the K-feldspar Microcline. *J. Phys. Chem. C*, 120(12):6704–6713, March 2016. ISSN 1932-7447. doi:10.1021/acs.jpcc.6b01155. URL <https://doi.org/10.1021/acs.jpcc.6b01155>.
- ⁸¹Arpa Hudait, Nathan Odendahl, Yuqing Qiu, Francesco Paesani, and Valeria Molinero. Ice-Nucleating and Antifreeze Proteins Recognize Ice through a Diversity of Anchored Clathrate and Ice-like Motifs. *J. Am. Chem. Soc.*, 140(14):4905–4912, April 2018. ISSN 0002-7863, 1520-5126. doi:10.1021/jacs.8b01246. URL <http://pubs.acs.org/doi/10.1021/jacs.8b01246>.
- ⁸²Rosalind J Allen, Chantal Valeriani, and Pieter Rein ten Wolde. Forward flux sampling for rare event simulations. *J. Phys. Cond. Matt.*, 21(46):463102, November 2009. ISSN 0953-8984, 1361-648X. doi:10.1088/0953-8984/21/46/463102. URL <http://stacks.iop.org/0953-8984/21/i=46/a=463102?key=crossref.8b23c2067b5af547525431d4897b94f6>.
- ⁸³Tianshu Li, Davide Donadio, Giovanna Russo, and Giulia Galli. Homogeneous ice nucleation from supercooled water. *Phys. Chem. Chem. Phys.*, 13(44):19807–19813, November 2011. ISSN 1463-9084. doi:10.1039/C1CP22167A. URL <http://pubs.rsc.org/en/content/articlelanding/2011/cp/c1cp22167a>.
- ⁸⁴Tianshu Li, Davide Donadio, and Giulia Galli. Ice nucleation at the nanoscale probes no man’s land of water. *Nat. Commun.*, 4:1887, May 2013. doi:10.1038/ncomms2918. URL <http://www.nature.com/ncomms/journal/v4/n5/full/ncomms2918.html#ref7>.
- ⁸⁵C. Valeriani, E. Sanz, and D. Frenkel. Rate of homogeneous crystal nucleation in molten NaCl. *J. Chem. Phys.*, 122(19):194501, May 2005. ISSN 0021-9606, 1089-7690. doi:10.1063/1.1896348. URL <http://scitation.aip.org/content/aip/journal/jcp/122/19/10.1063/1.1896348>.
- ⁸⁶Zun-Jing Wang, Chantal Valeriani, and Daan Frenkel. Homogeneous Bubble Nucleation Driven by Local Hot Spots: A Molecular Dynamics Study. *J. Phys. Chem. B*, 113(12):3776–3784, March 2009. ISSN 1520-6106. doi:10.1021/jp807727p. URL <http://dx.doi.org/10.1021/jp807727p>.
- ⁸⁷Yuanfei Bi and Tianshu Li. Probing Methane Hydrate Nucleation through the Forward Flux Sampling Method. *J. Phys. Chem. B*, 118(47):13324–13332, November 2014. ISSN 1520-6106. doi:10.1021/jp503000u. URL <http://dx.doi.org/10.1021/jp503000u>.
- ⁸⁸Melisa M. Gianetti, Amir Haji-Akbari, M. Paula Longinotti, and Pablo G. Debenedetti. Computational investigation of structure, dynamics and nucleation kinetics of a family of modified Stillinger-Weber model fluids in bulk and free-standing thin films. *Phys. Chem. Chem. Phys.*, 18(5):4102–4111, January 2016. ISSN 1463-9084. doi:10.1039/C5CP06535F. URL <http://pubs.rsc.org/en/content/articlelanding/2016/cp/c5cp06535f>.
- ⁸⁹Amir Haji-Akbari and Pablo G. Debenedetti. Computational investigation of surface freezing in a molecular model of water. *Proc. Natl. Acad. Sci. U.S.A.*, 114(13):3316–3321, March 2017. ISSN 0027-8424, 1091-6490. doi:10.1073/pnas.1620999114. URL <http://www.pnas.org/content/114/13/3316>.
- ⁹⁰Alessandro Laio and Michele Parrinello. Escaping free-energy minima. *Proc. Natl. Acad. Sci. U.S.A.*, 99(20):12562–12566, 2002.
- ⁹¹P. G. Bolhuis, D. Chandler, C. Dellago, and P. L. Geissler. Transition path sampling: Throwing ropes over rough mountain passes, in the dark. *Annu. Rev. Phys. Chem.*, 53:291–318, 2002.
- ⁹²J. R. Espinosa, C. Vega, C. Valeriani, and E. Sanz. Seeding approach to crystal nucleation. *J. Chem. Phys.*, 144(3):034501, 2016.
- ⁹³Amir Haji-Akbari. Forward-flux sampling with jumpy order parameters. *J. Chem. Phys.*, 149(7):072303, August 2018. ISSN 0021-9606, 1089-7690. doi:10.1063/1.5018303. URL <http://aip.scitation.org/doi/10.1063/1.5018303>.
- ⁹⁴Gareth A. Tribello, Federico Giberti, Gabriele C. Sosso, Matteo Salvalaglio, and Michele Parrinello. Analyzing and Driving Cluster Formation in Atomistic Simulations. *J. Chem. Theory Comput.*, 13(3):1317–1327, March 2017. ISSN 1549-9618, 1549-9626. doi:10.1021/acs.jctc.6b01073. URL <http://pubs.acs.org/doi/10.1021/acs.jctc.6b01073>.

- ⁹⁵Martin Fitzner, Gabriele C. Sosso, Fabio Pietrucci, Silvio Pipolo, and Angelos Michaelides. Pre-critical fluctuations and what they disclose about heterogeneous crystal nucleation. *Nat. Commun.*, 8(1):2257, December 2017. ISSN 2041-1723. doi:10.1038/s41467-017-02300-x. URL <http://www.nature.com/articles/s41467-017-02300-x>.
- ⁹⁶Raffaella Cabriolu and Tianshu Li. Ice nucleation on carbon surface supports the classical theory for heterogeneous nucleation. *Phys. Rev. E*, 91(5):052402, May 2015. doi:10.1103/PhysRevE.91.052402. URL <http://link.aps.org/doi/10.1103/PhysRevE.91.052402>.
- ⁹⁷Emily B. Moore and Valeria Molinero. Is it cubic? Ice crystallization from deeply supercooled water. *Phys. Chem. Chem. Phys.*, 13(44):20008, 2011. ISSN 1463-9076, 1463-9084. doi:10.1039/c1cp22022e. URL <http://pubs.rsc.org/en/content/articlehtml/2011/cp/c1cp22022e>.
- ⁹⁸T. C. Hansen, M. M. Koza, P. Lindner, and W. F. Kuhs. Formation and annealing of cubic ice: II. Kinetic study. *J. Phys. Cond. Matt.*, 20(28):285105, 2008. ISSN 0953-8984. doi:10.1088/0953-8984/20/28/285105. URL <http://stacks.iop.org/0953-8984/20/i=28/a=285105>.
- ⁹⁹Tamsin L. Malkin, Benjamin J. Murray, Christoph G. Salzmann, Valeria Molinero, Steven J. Pickering, and Thomas F. Whale. Stacking disorder in ice I. *Phys. Chem. Chem. Phys.*, 17(1):60–76, December 2014. ISSN 1463-9084. doi:10.1039/C4CP02893G. URL <http://pubs.rsc.org/en/content/articlelanding/2015/cp/c4cp02893g>.
- ¹⁰⁰D. O’Sullivan, B. J. Murray, J. F. Ross, T. F. Whale, H. C. Price, J. D. Atkinson, N. S. Umo, and M. E. Webb. The relevance of nanoscale biological fragments for ice nucleation in clouds. *Sci. Rep.*, 5:8082, January 2015. ISSN 2045-2322. doi:10.1038/srep08082. URL <http://www.nature.com/srep/2015/150128/srep08082/full/srep08082.html>.
- ¹⁰¹S. Augustin, H. Wex, D. Niedermeier, B. Pummer, H. Grothe, S. Hartmann, L. Tomsche, T. Clauss, J. Voigtlander, K. Ignatius, and F. Stratmann. Immersion freezing of birch pollen washing water. *Atmospheric Chem. Phys.*, 13(21):10989–11003, November 2013. ISSN 1680-7316. doi:<https://doi.org/10.5194/acp-13-10989-2013>. URL <https://www.atmos-chem-phys.net/13/10989/2013/>.
- ¹⁰²P. Pedevilla, M. Fitzner, G. C. Sosso, and A. Michaelides. Heterogeneous seeded molecular dynamics as a tool to probe the ice nucleating ability of crystalline surfaces. *J. Chem. Phys.*, 2018. Submitted.